

Characterization of cohesive granular flow morphology

Fanshuo Ma^{1,*}, Pierre-Yves Lagrée^{1,**}, and Lydie Staron^{1,***}

¹Sorbonne Université, CNRS, Institut Jean le Rond d'Alembert, F-75005 Paris France

Abstract. We simulate cohesive granular flows over an inclined plane using the 2D Contact Dynamics algorithm. The plug thickness is measured from numerical simulations considering various adhesive contact strengths. Flow surface roughness is investigated by calculating the fluctuation of surface topography. The distribution of fluctuation intensity across different adhesive strengths is also discussed. Roughness correlation on flow surface is studied using a pair correlation function applied to the positions of surface grains. A characteristic length is defined from the correlation results, considering both cohesive and non-cohesive cases. A quantitative comparison is conducted with a recent experimental study that relates the characteristic length to the agglomeration size in cohesive granular flows.

1 Introduction

The presence of attractive forces among grains can significantly alter the physical properties of granular flows, for instance, through the formation of capillary bridges [1]. The Bagnold velocity profile [2], which characterizes non-cohesive flows, no longer holds in the presence of adhesive inter-particle contacts. Instead, a plug region emerges near the surface [3]. Also, the formation of grain agglomerates can alter the mesoscopic morphological characteristics of the flow. By analysing the fracture profiles during the cracking of cohesive granular materials under controlled atmospheric humidity, *Tapia et al* [4] observed that the size of grain clusters increases with humidity. *Abramian et al* [5] investigated the rough surface of cohesive granular deposit using discrete simulation method. They found that the surface roughness correlates with inter-particle adhesive forces, exhibiting self-affine scaling behaviour. *Deboeuf et al* [6] estimated the agglomerate size in the cohesive inertial flow by comparing experimental mass flow rate data to theoretical predictions, incorporating the grain aggregate size into the cohesive flow model. While most of these studies focus on cohesive granular systems in quasi-static states, investigating the role of adhesion in the morphology of rapid chute flows is both pertinent and valuable.

Granular flow down an inclined plane driven by gravity is simulated with 2D discrete numerical method and the steady uniform flow morphology is investigated through three aspects: the thickness of the plug region, the roughness of the free surface, and the spatial correlation of surface roughness with the distance between two grains on the surface.

2 Numerical Experiment

Numerical simulations in our work are performed using an in-house 2D Contact Dynamics (CD) algorithm. Contact forces between grains are resolved based on their relative velocities at contact, using a regularized Signorini contact law combined with an Amontons-Coulomb friction law as complementary contact laws. Additionally, adhesive forces arise when grains come into contact, characterized by the maximum adhesive force: $F_c = Bo_g m_{ij} g$, where Bo_g is the granular Bond number, m_{ij} is the reduced mass of two contacting grains, and g is the gravitational acceleration. The contact friction is determined based on a modified Coulomb law: $F_t = \mu_{gg}(F_n + F_c)$, where $\mu_{gg} = 0.2$ is the inter-grain friction coefficient and F_n is the normal contact force. A comprehensive description of CD algorithm is presented in [7].

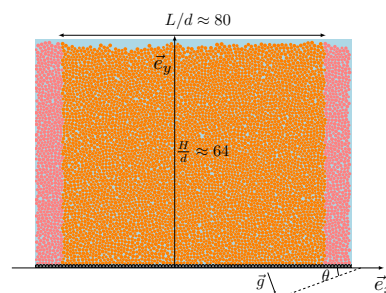


Figure 1. Schematic simulation of a granular system containing 5280 grains of length $L \approx 80d$, with system height $H \approx 64d$. Grains coloured in orange represent the moving particles in the granular flow and rose-coloured grains on the sides are periodic images of the orange grains, illustrating the use of periodic boundary conditions. Gravity is applied at an angle θ from the vertical to mimic the conditions of an inclined plane.

*e-mail: fanshuo.ma@upmc.fr

**e-mail: pierre-yves.lagree@upmc.fr

***e-mail: lyd.staron@gmail.com

The granular system simulated comprises 5280 perfect rigid grains with diameters uniformly distributed in $[d_{min}, d_{max}]$ with $d_{max}/d_{min} = 1.5$ and mean diameter $d = 0.005\text{ m}$. The system is initially generated by free falling grains under reduced gravity, arranged in a regular hexagonal mesh. Upon reaching a final static state, the packing forms a system with a length of $L \approx 80d$ and a height of $H \approx 64d$ as shown in figure 1. The system is then tilted at an angle θ with respect to the horizontal to induce flow. The results reported in our work are measured under steady, uniform flow conditions, indicated by a steady system kinetic energy profile.

3 Measurement of Plug Region

The plug region refers to the area where no velocity shear is present, allowing us to visualize and measure it from the flow velocity profile. In figure 2 we present the mean velocity profile extracted from numerical simulations for various tilt angle θ and granular Bond numbers Bo_g under steady uniform flow conditions. We notice that as Bo_g increases, the plug region emerges.

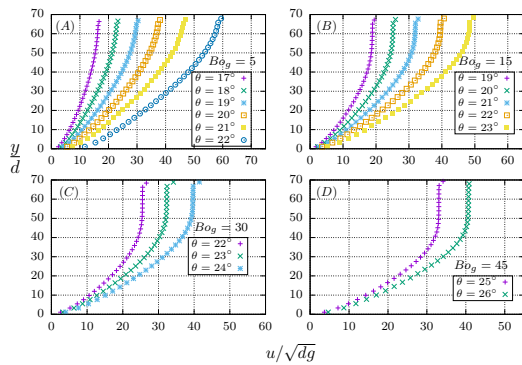


Figure 2. Velocity profiles for cohesive flows over an inclined plan. Cohesion is characterized by the granular Bond number Bo_g . (A): $Bo_g = 5$; (B): $Bo_g = 15$; (C): $Bo_g = 30$; (D): $Bo_g = 45$. At each Bo_g , a steady uniform flow can be established on the plane at different tilt angles θ .

To measure the plug thickness H_c , we first compute the spatial and temporal averages of the velocity profile along the depth in a stationary steady flow. Previous studies have presented typical mean velocity profiles exhibiting the existence of a plug region through discrete numerical simulations [3, 8]. In this work, H_c is determined from the position where the local velocity gradient $\dot{\gamma}$ reaches zero. However the exact position where $\dot{\gamma} = 0$ is not clearly defined. Therefore, we need to establish a cutoff value for $\dot{\gamma}$ to distinguish plug region from the flow region where a noticeable velocity gradient appears.

Numerically, the velocity field is discretised into layers, and we define the local relative velocity variation be-

tween two adjacent layers as:

$$\left(\frac{\Delta V}{V}\right)_l = \frac{V_{l+1} - V_l}{V_l}, \quad (1)$$

where V_l denotes the time- and space-averaged velocity at layer l . We define Y_c as the lowest vertical position where the relative velocity variation $\Delta V/V = 0.01$. The plug thickness H_c is then computed as $H_c = H - Y_c$, where H is the total flow thickness.

In figure 3, we present the plug thickness H_c measured from the discrete numerical simulations. For a given granular Bond number Bo_g , the plug thickness decreases with increasing plane inclination θ . Conversely, for a fixed tilt angle θ , the plug thickness increases with increasing Bo_g .

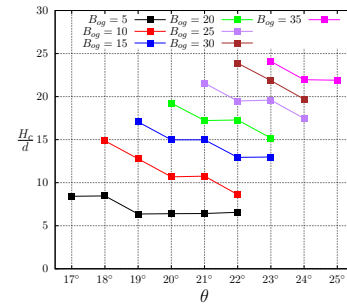


Figure 3. Thickness of plug region H_c as a function of Bo_g and tilt angle θ .

The presence of a solid-like region within the flow reflects the plastic behavior of cohesive granular materials: shear stress must exceed a threshold for flow to initiate. As the tilt angle increases, the flow experiences greater shear stress in the steady state, particularly along the flow direction. Consequently, the yield stress is reached at a higher position within the material, leading to a decrease in plug thickness with increasing tilt angle θ . Conversely, strengthening the adhesive contact forces, by increasing the granular Bond number Bo_g , allows grains to bond more firmly, forming a solid-like structure that can withstand higher shear stresses without yielding. As a result, the plug thickness increases with increasing Bo_g .

4 Flow Surface Roughness

In our 2D flow model, surface roughness is analysed based on the fluctuation of surface grains positions relative to the spatial mean level. In non-cohesive flows, where flow instability may play a significant role [9], these fluctuations can arise from grain motion or surface deformation. In contrast, for cohesive granular systems, the roughness observed on the grain flow surface is primarily attributed to the formation of clusters due to adhesive forces among grains [5].

In figure 4, we present four snapshots illustrating the flow surface at different tilt angle θ and adhesive contact strengths characterized by the granular Bond number

Bo_g . In these visualizations, surface grains are depicted in black. We observe that as Bo_g increases, the surface roughness becomes more pronounced, indicating that adhesive forces contribute significantly to the fluctuation of grain positions on the flow surface.

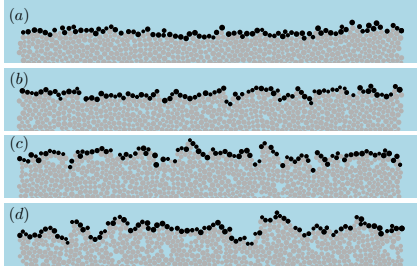


Figure 4. Snapshots of the flow surface with surface grains highlighted in black. (a) : $Bo_g = 0, \theta = 16^\circ$; (b) : $Bo_g = 15, \theta = 20^\circ$; (c) : $Bo_g = 30, \theta = 24^\circ$; (d) : $Bo_g = 50, \theta = 26^\circ$.

To characterize the surface roughness of the flow, we first compute the space average of the free surface profile at each instant after the steady, uniform regime is established, yielding $\bar{h}(t)$. The surface fluctuation $\eta(x, t)$ is then obtained by subtracting the spatially averaged profile $\bar{h}(t)$ from the instantaneous surface profile $h(x, t)$, as defined by equation 2:

$$\eta(x, t) = h(x, t) - \bar{h}(t). \quad (2)$$

The behaviour of function $\eta(x, t)$ provides an estimate of the surface roughness level, as it represents deviations of the surface position from the mean level. In the following analysis, we assume that the flow occurs over a sufficient long plane and neglect spatial correlations in the fluctuations. Under these assumptions, we define $\eta = \{y|y \in \bigcup_{x,t} \eta(x, t)\}$, representing the ensemble of surface deviations over space and time.

To further characterize flow surface fluctuations, we examine the probability distribution function (PDF) of η . In figure 5 we present the PDFs corresponding to the four flows whose surface profiles are presented in figure 4. The shape of the PDF provides insight into the amplitude of the surface fluctuations: a taller and narrower PDF indicates that the majority of fluctuations are of smaller amplitude, whereas a broader and flatter PDF reflects the presence of larger-amplitude fluctuations. The results show that surface fluctuation increases with the adhesive contact strength Bo_g , which is coherent with the observation in figure 4. Additionally, we find that the PDFs of η are well approximated by Gaussian distribution. This allows the use of classical statistical parameters, such as the standard deviation, to quantify surface roughness.

A natural next step is to investigate how the standard deviation σ , which is directly related to the width of the Gaussian distribution, varies with the tilt angle θ and adhesive contact strength Bo_g . In figure 5, we plot the evolution of σ as a function of θ for different values of Bo_g .

For non-cohesive flows, σ increases with the tilt angle θ , meaning the increase in surface fluctuation amplitude

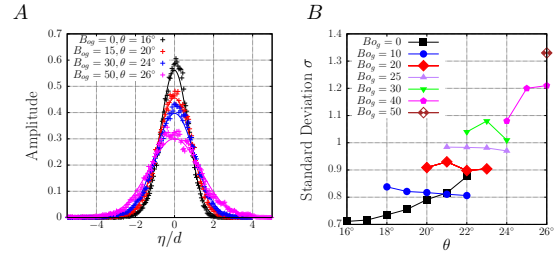


Figure 5. (A): Probability density function (PDF) of surface fluctuation η . A Gaussian distribution, $f(x) = \frac{1}{\sigma\sqrt{2\pi}} \exp(-\frac{(\eta-\bar{\eta})^2}{2\sigma^2})$, is used to fit the data, where $\bar{\eta}$ and σ denote the mean and standard deviation of η . (B): Standard deviation of η as a function of Bo_g and θ .

as θ rises. This trend may suggest a link between the enhancement of surface fluctuations and the onset of an instability mode, as proposed in previous studies [9]. However a dedicated investigation is required to fully explore and validate this hypothesis.

When adhesive contact between grains is significant, the surface morphology exhibits a different behaviour. Stronger adhesive interactions can lead to rougher surface during fracture [4] and in slumping deposits [5], primarily due to the formation of larger clusters or aggregate. This mechanism likely explains the observed increase in σ with adhesive strength Bo_g . In contrast, variations in the inclination angle θ appear to have only a minor effect on σ . Since the flow surface corresponds to the plug region, where grains are bounded through adhesive forces, the adhesive contact strength becomes the dominant factor influencing surface roughness.

5 Surface Roughness Correlation

We now turn to the analysis of flow surface roughness correlations. To this end, we employ a pair correlation function, as defined in equation 3. This type of two-point correlation function has been previously used to investigate velocity correlations in both surface and bulk region regions of gravity-driven dense granular flows [10, 11]. In our case, since we are specifically interested in correlation of surface fluctuation, equation 3 is applied to compute the spatial correlation of η along the x -direction.

$$K(r) = \frac{\sum_t \left[\sum_{i=1}^{N_s-1} \sum_{j=i+1}^{N_s} \eta(x_i, t) \eta(x_j, t) \Pi(r - r_{ij}) \right]}{\sum_t \left[\sum_{i=1}^{N_s-1} \sum_{j=i+1}^{N_s} \Pi(r - r_{ij}) \right]}, \quad (3)$$

where $\Pi(x)$ is a step function that takes the value 1 when $|x/d| < 0.5$ and 0 otherwise. N_s denotes the number of grain position located on the flow surface, while r_{ij} represents the distance between grains i and j . The correlation is computed over multiple time instants t within the steady flow regime.

We first present the results of equation 3 applied to the surface of non-cohesive flow, as shown in figure 6. As

the inclination angle θ increases, the correlation function $K(r)$ decays more slowly, indicating enhanced spatial correlation of surface fluctuations. To quantify this effect, we define the characteristic correlation length l_x such that $K(l_x)/K(d) = 0.1$. A similar definition is used in [10]. At $K(l_x) = 0.1K(d)$, we consider that no significant spatial correlation exists on the flow surface between two grains separated by the distance l_x . The evolution of l_x with respect to tilt angle θ is plotted in figure 6. The results show that, for flows on steeper planes, surface grains exhibit long-range correlations, suggesting that surface structures extend over greater distances.

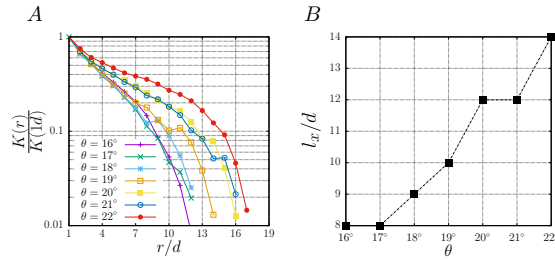


Figure 6. (A) Pair correlation function $K(r)$ of flow surface fluctuation in non-cohesive flow at various tilt angle θ , normalized by the value at $r = d$. The horizontal axis r is expressed in mean grain diameter. (B): Characteristic correlation length l_x , defined by $K(l_x)/K(d) = 0.1$, plotted as a function of the tilt angle θ .

The picture changes noticeably when adhesive contact is taken into account. In the figure 7, we present the results of correlation function applied to steady cohesive flow surfaces.

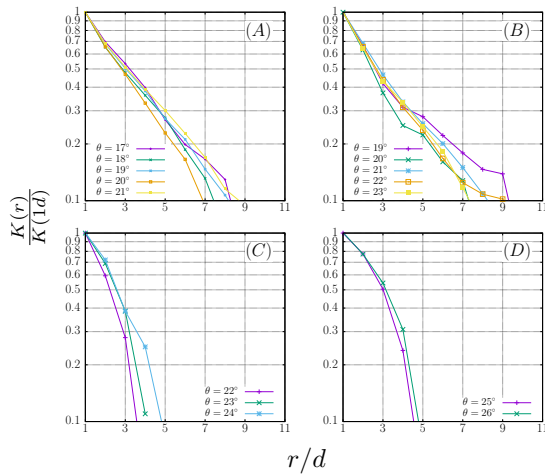


Figure 7. Pair correlation function $K(r)$ of surface fluctuation in cohesive flow at various tilt angle θ , normalized by the value at $K(r = d)$. The horizontal axis r is expressed in mean grain diameter. (A) $Bo_g = 5$; (B) $Bo_g = 15$; (C) $Bo_g = 30$; (D) $Bo_g = 45$.

We observe that the tilt angle θ has minimal influence on the correlation length l_x and l_x decreases with increasing Bo_g . This trend can be attributed to the increasing of roughness higher Bo_g as observed in Sec. 4, which reduce the spatial extent over which grains remain correlated. For cohesive flows, surface roughness primarily results from the formation of agglomerates. This interpretation is supported by the experimental work of Deboeuf *et al* [6], who estimated the grain aggregate sizes in the range $d_{agg}/d \in [4, 9]$. The correlation length l_x measured in our study for cohesive flows are in quantitative agreement with these aggregate size estimates, reinforcing the role of agglomeration in shaping surface morphology under cohesive conditions.

6 Conclusion

The morphology of cohesive granular flows has been analyzed in terms of surface plug thickness H_c , surface roughness, and the corresponding spatial correlation. Consistent qualitative trends are obtained for the plug region thickness: H_c decreases with increasing plane inclination and increases with adhesive contact strength. Regarding surface roughness, we find that it is well described by a Gaussian distribution, with the standard deviation strongly influenced by adhesion strength Bo_g , but only marginally affected by the tilt angle θ .

While the present study focuses on 2D simulations, extending this work to 3D remains an important direction for future work. In 3D, adhesive contacts transverse to the flow may become significant and the system geometry also play a crucial role in the material dynamics (see Pol *et al* [12]). Investigating how the plug thickness, surface roughness would change with inter-particle adhesive strength in 3D provide a more comprehensive understanding of cohesive free-surface flow morphology under realistic conditions.

References

- [1] M. Namiko, and F. Nori. (2006). *Advances in Physics* 55 (1–2): 1–45.
- [2] GDR Midi. (2004). *Eur. Phys. J. E* 14, 341–365.
- [3] R. Brewster, G. S. Grest, J. W. Landry, and A. J. Levine. (2005). *Phys. Rev. E* 72, 061301.
- [4] F. Tapia, S. Santucci, and J.-C. Géminard. (2016). *Europhysics Letters* 115, 64001.
- [5] A. Abramian, P.-Y. Lagrée, and L. Staron. (2021). *Soft Matter* 17, 10723.
- [6] S. Deboeuf and A. Fall. (2023). *Journal of Rheology*.
- [7] F. Radjai and V. Richefeu. (2009). *Mechanics of Materials* 41, 715.
- [8] P. G. Rognon, J.-N. Roux, M. Naaim, and F. Chevoir. (2008). *Journal of Fluid Mechanics* 596, 21–47.
- [9] Y. Forterre, O. Pouliquen. (2001). *Phys. Rev. Lett.*
- [10] O. Pouliquen. (2004). *Phys. Rev. Lett.* 93, 248001.
- [11] L. Staron. (2008). *Phys. Rev. E* 77, 051304.
- [12] Pol, R. Artoni, P. Richard (2025). *J. Fluid. Mech.*